Simulation of Geomechanical Behavior during SAGD Process using COMSOL Multiphysics®

X. Gong[1], R.Wan[*2]
Department of Civil Engineering, University of Calgary, Calgary, Alberta, Canada.
*Corresponding author: 2500 University Dr. NW, Calgary, Alberta, Canada.
Email: wan@ucalgary.ca

Abstract: Steam-Assistant-Gravity-Drainage (SAGD) has become one of the most commonly used thermal recovery processes to extract heavy oil from oil sand reservoirs, especially in Northern Alberta, Canada. However, due to geological history, interbedded shales (IBS) in the reservoir act as barriers due to their low permeability and as such hinder the progression of the steam chamber. Cap-rock integrity also needs to be ensured to prevent steam breakthrough. Therefore, a comprehensive investigation of coupling between thermal multiphase fluid flow and geomechanics is required in modeling SAGD processes to properly address the above issues.

In this paper, the THM behavior of the heavy oil reservoir was studied through a proper constitutive modeling of the porous media. Both homogeneous and non-homogeneous reservoir conditions were investigated based on stress path and stress/strain field analyses.

Keywords: SAGD, Cap-Rock, Interbedded Shale (IBS), Thermo-ElastoPlastic Constitutive Model

1. Introduction

Steam-Assisted-Gravity-Drainage (SAGD) is one of the most effective thermal recovery methods used to recover heavy oil from oil sand reservoirs of Northern Alberta, Canada. This process involves the injection of steam at high temperature (225°C) into the oil sand formation through an upper injection horizontal well, with a lower horizontal well acting as the producer. Basically, the mechanism is such that, as steam condenses in contact with the surrounding formation it transfers heat to the latter thereby significantly reducing the viscosity of heavy oil in the pore space. As a result, the heated heavy oil with higher mobility will flow under gravity into the lower production well.

Numerous theoretical and numerical studies based on so-called dead oil model, black oil model, compositional model, among others, have been conducted following well-established multiphase fluid flow theory. For instance, Shutler (1969, 1970) studied a three-phase dead oil model and applied to the steamflooding strategy. Jensen (1991) developed a steamflooding simulator using a simple three-phase and two-component dead oil model to study fractured reservoir. Hansamuit (1990) also developed a three-dimensional compositional simulator to investigate steam injection process. However, all the above-mentioned studies focus on well-established reservoir simulation without considering important geomechanical effects. On the other hand, it is well-known that steam injection during SAGD process significantly alters both pore fluid pressure and temperature fields, which in turn affects the effective or skeleton stress in the reservoir. As such, geomechanical effects and multiphase fluid flow are tightly intertwined and this coupling needs to be systematically considered in any numerical simulation of SAGD, especially if material failure is one of the important issues to be investigated.

In this paper, the main objective is to investigate the geomechanical behavior of oil sand and interbedded shale (IBS) during SAGD process using an advanced constitutive model. Specifically, plastic deformations, dilation and potential unstable failure conditions of both oil sand and shale during the SAGD process are evaluated through the respective stress strain relationships and an effective stress path analysis. In addition, localization and material instability phenomenon (Wan, et al. 2011, Wan, et al. 2012) are also studied. A generalized density-stress-fabric dependent elasto-plastic (so-called WG) model initially developed by Wan and Guo (1998) is employed in this paper to show the relevance of geoemechanics and how it is effectively used to evaluate material failure issues in SAGD process with IBS.

2. Mathematical Formulation

In this section, the physical process of coupling non-isothermal multiphase fluid flow with geomechanical deformation and stress in the reservoir is mathematically formulated following basic balance laws. For multiphase fluid flow, mass and energy conservation equations are advocated, whereas for geomechanics, Biot's consolidation (Biot, 1941) type of quasi-static equilibrium formulation with elasto-plastic constitutive relation is used. As for the elasto-plastic constitutive relation, a density-stress-fabric dependent elasto-plastic (WG) model initially developed by Wan and Guo (1998) and generalized thereafter is briefly summarized.

2.1 Assumption

It is important to recall some assumptions that are made for the derivation of the current coupled multiphase flow and geomechanics model, i.e.

- Three phase (water, oil and gas) and two components (water and oil) dead oil model is assumed;
- Capillary pressure is ignored;
- Local thermodynamic equilibrium is assumed;
- Darcy's law and small strains are assumed.

2.2 Multiphase fluid equations

Water mass balance:

$$\frac{\partial}{\partial t}\left(\phi\rho_w S_w + \phi\rho_g S_g\right) = -\nabla\cdot\left(\phi\rho_w S_w \mathbf{v}_w + \phi\rho_g S_g \mathbf{v}_g\right) + q_w + q_g$$

Oil mass balance:

$$\frac{\partial}{\partial t}\left(\phi\rho_o S_o\right) = -\nabla\cdot\left(\phi\rho_o S_o \mathbf{v}_o\right) + q_o$$

Darcy's law:

$$\mathbf{v}_{d\alpha} = -K\frac{k_{r\alpha}}{\mu_\alpha}\left(\nabla p_\alpha - \rho_\alpha g \nabla Z\right) \quad \alpha = w,o,g$$

Energy balance:

$$\frac{\partial}{\partial t}\left[(1-\phi)\rho_s U_s + \phi\sum_{\alpha=w,o,g}\left(\rho_\alpha S_\alpha U_\alpha\right)\right] = \nabla\cdot\left(\lambda_{pm}\nabla T\right) - \nabla\cdot\left[\begin{array}{l}(1-\phi)\rho_s H_s \mathbf{v}_s + \\ \phi\sum_{\alpha=w,o,g}\left(\rho_\alpha S_\alpha H_\alpha \mathbf{v}_\alpha\right)\end{array}\right]$$

Saturation constraint:

$$S_w + S_o + S_g = 1$$

2.3 Geomechanics

Equilibrium equation:

$$\frac{\partial\sigma_{ij}}{\partial x_j} + b_i = 0$$

Principle of effective stress:

$$\sigma_{ij}^{'} = \sigma_{ij} + \alpha\, p_{avg}\delta_{ij}$$

Stress strain relation:

$$\sigma_{ij}^{'} = \mathbf{D}^{ep}\left(\varepsilon_{ij} - \varepsilon_{ij}^{th} - \varepsilon_{ij}^{0}\right)$$

2.4 Elasto-Plastic Constitutive Law

Here, the generalized density-stress-fabric dependent WG model is used to evaluate the granular geomaterial behavior. The yielding function is derived from multi-surface plasticity and Critical State theory, with flow rule derived from Rowe's stress dilatancy theory (Rowe, 1962). The basic formulation is summarized below.

Yielding Function:

$$F = q - Mp$$

where M is the slope of yielding surface in $p-q$ plane which can be written as:

$$M = \frac{6\sin\phi_m}{3-\sin\phi_m}$$

with ϕ_m as the mobilized friction angle.

Hardening/Softening Law:

$$\sin\phi_m = \frac{\gamma_p}{\alpha_0 + \gamma_p}\left(\frac{e}{e_{cs}}\right)^{-n_m}\sin\phi_{cs}$$

where γ_p is the deviatoric plastic strain; e is the current void ratio; e_{cs} is the critical void ratio; ϕ_{cs} is the critical state friction angle; α_0 and n_m are material properties.

Plastic Potential:

$$G = q - \sin\psi_m p$$

where ψ_m is the mobilized dilatancy angle expressed by:

$$\sin\psi_m = \frac{\sin\phi_m - \sin\phi_f}{1 - \sin\phi_m \sin\phi_f}$$

3. Numerical Studies

The main focus here is to study geomechanical behaviors of oil sand and interbedded shale (IBS), and their influence on the SAGD process under a fully coupled fluid flow and reservoir deformation finite element analysis. Three main case studies have been simulated and systematically compared as follows: (1) Homogeneous reservoir using Mohr-Coulomb model as constitutive law for oil sand reservoir; (2) Homogeneous reservoir using WG model as constitutive law for oil sand reservoir; and (3) Randomly distributed inclined IBS using WG model for both oil sand and IBS. Various aspects of the computations are discussed, namely: effective stress paths at strategic points in the reservoir, and plastic shear strain levels and potential localization, including unstable material zones. Both temporal and spatial maps of the various above-mentioned features enhance the understanding of the geomechanical behavior of the reservoir under a thermo-hydro-mechanical setting, especially in the presence of IBS.

Figure 1 shows the general configuration of the finite element simulation as well as the initial and boundary condition. Strategic points A to F are chosen within the reservoir to follow the evolution of various controlling field variables. Four interbedded shale (IBS) intrusions, 20 m long and 1 m thick inclined at 10° to the horizontal, are placed hypothetically within the reservoir. The finite element mesh comprised of 3850 and 64,140 quadratic elements for the homogeneous reservoir and the IBS embedded case respectively. For the COMSOL modeling, the user defined PDE's are the most suitable modules for this highly coupled and nonlinear problem. The numerical simulation of the SAGD process span over a period of 2.5 years approximately.

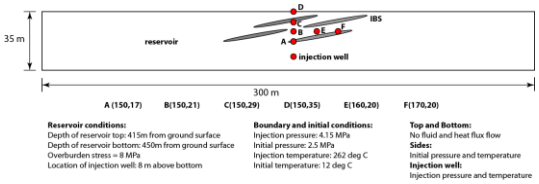

Figure 1: SAGD simulation configuration and operation conditions (figure not to scale)

3.1 Stress Path and Stress Strain

Figures (2a) and (2b) show the effective stress paths followed by strategic points A-F in the reservoir as computed using MC and WG models, respectively. For MC model, the effective stress paths initially turn to the left with decreasing effective mean stress and increases in deviatoric stress as a result of an upsurge in pore fluid pressures for points A-D located above the well. At this stage, the effect of pressure is dominant due to faster pressure propagation relative to that of temperature. However, after about 200 days, the effect of temperature significantly comes into play as deviatoric stresses increase mainly because of the thermal expansion and the confinement of the reservoir. The strength of material is ultimately reached at the plastic limit whereby the effective stress path essentially tangents the Mohr-Coulomb failure envelope; see **Figure (2a)**. Large plastic strains are thus developed due to material failure as illustrated in the stress strain plots in **Figure (2c)** where a slight increase in deviatoric stress causes large increases in plastic shear strain. As temperatures further rise within the reservoir, mean effective stresses can only increase, making the stress path deviate from the failure envelope. For points E and F which are located away from the central axis of the well, 'unloading' of deviatoric stresses occurs due to the fact that thermal expansion makes the horizontal stress increase at these points, thus causing the deviatoric stress to decrease from its initial value.

Turning to the WG model results, see **Figure (2b)**, similar initial behavior is observed for points A to D initially. However, similarities stop here since both effective stress paths and stress strain behaviors are very different from the MC case after the initial part. This is because of distinctive features of the WG model that incorporates progressive mobilization of dilatancy through strain hardening and softening,

among others. As the effective stress path reaches a certain level consistent with the peak strength of the material, it turns back to the left again with a reduction in deviatoric stress. The Critical State Line shown in **Figure (2b)** represents an ultimate state at which the critical state friction angle is $25°$, an intrinsic material strength parameter for oil sand. From the stress strain plot (**Figure (2d)**), it can be seen that material points A to C are subjected to an initial strain hardening phase followed by strain softening after a peak has been reached. This is a very typical behavior of geomaterials and oil sand whereby dense granular materials dilate and exhibit peak strength followed by strain softening around which point, unstable material behavior occurs through strain localization (see Wan, et al. 2012). The MC model does not contain the basic ingredients to capture such phenomena.

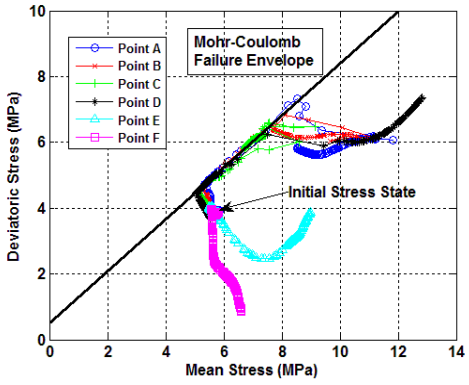

(a)

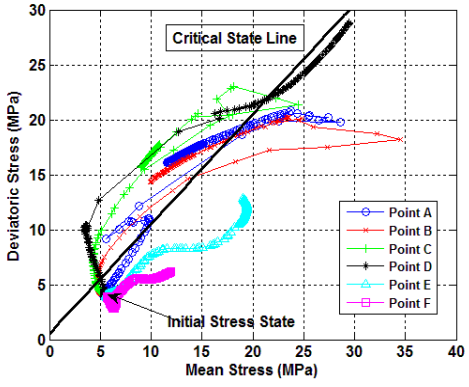

(b)

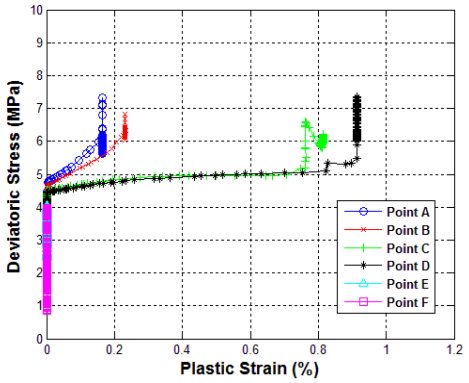

(c)

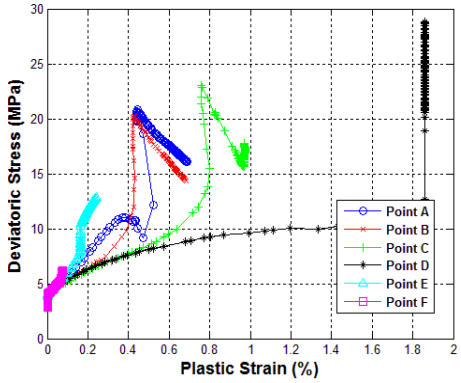

(d)

Figure 2: Effective stress path, stress strain and volumetric strain comparison for MC and WG models: (a) Stress path for MC model; (b) Stress path for WG model; (c) Stress strain for MC model; (d) Stress strain for WG model

3.2 Plastic Strain and Strain Localization

Figures (3a) and **(3b)** give the set of plots of temperature and plastic strain at some particular times. It can be found that before the steam chamber touches the top of the reservoir, the maximum plastic shear strain front is slightly ahead of temperature. Banded shear zones with large plastic shear strains are formed along a "V" shaped configuration. Thus, it can be concluded that potential localization failure and material instability zones are highly possible in these "V" shaped shear banded zones which emanate from the shoulders of the steam chamber at the reservoir top.

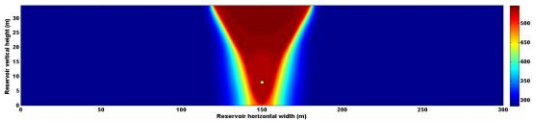

(a) Temperature at 167 days

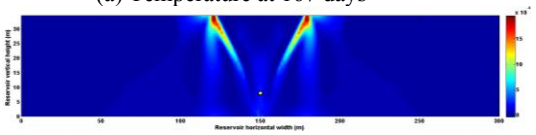

(b) Plastic shear strain from 120 to 167 days

Figure 3: Temperature, incremental plastic shear strain and second order work plots at various times for WG model

3.3 Interbedded shale case

Figures (4a) and **(4b)** show, respectively, the temperature field plots at 1080 days and the incremental plastic shear strain field at a particular time increment for non-homogeneous reservoir case. Although the IBS has extremely low permeability and porosity, the propagation of steam and temperature is not completely blocked by the IBS, but advances with a slight degree of penetration into the IBS. However, the propagation of both fluid flow and temperature is postponed, thereby slowing the progress of heating in the formation in contrast to the homogeneous reservoir case. Herein, the difference in permeability between oil sand and IBS is about 6 orders of magnitude. Such a large difference makes both the steam and temperature to evolve through the gap between IBS in the reservoir and ultimately form the "zig-zag" flow pattern.

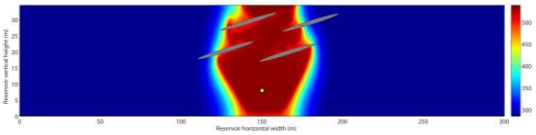

(a) Temperature at 1080 days

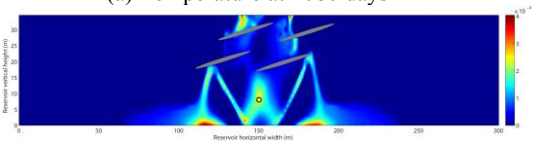

(b) Plastic shear strain from 996 to 1080 days

Figure 4: Temperature, incremental plastic shear strain and second order work plots at various times for WG model

4. Conclusions

The paper provides a comprehensive analysis of material failure in a reservoir under SAGD process from a fully coupled geomechanics and multiphase fluid flow setting. Among other things, the intent is to highlight the display of rich geomechanical features afforded by the use of a comprehensive constitutive model. The essential findings of the paper can be summarized as follows.

- The comprehensive and robust elasto-plastic constitutive WG model is capable to capture the complex stress strain response of oils and and shale. Linear/non-linear elasticity or elastic-perfectly plastic Mohr-Coulomb models severely hampers their use in analyzing geomechanics in SAGD process.
- Strain localization failure modes and potentially unstable material behavior were successfully simulated using the WG model.
- Results of the IBS reservoir simulation show a meandering flow pattern around the IBS due to the extremely low permeability and porosity of the shale. The blocking of steam flow by the IBS postpones the whole SAGD operation when compared with the homogeneous reservoir case.

5. Acknowledgements

This work is jointly funded by the Computer Modelling Group (CMG) and the Natural Science and Engineering Council of Canada (NSERC) through a CRD grant. The authors also thank CMG Ltd. for generous support in the form of free access to man-hours and STARS software.

6. References

1. Biot, M.A., "General theory of three-dimensional consolidation". Journal of Applied Physics, Vol. 12, pp. 155-164. (1941)
2. COMSOL Multiphysics. COMSOL Multiphysics User Guide (Version 4.3a), COMSOL, AB. (2012)
3. Hansamuit, V., "The development and application of a three-dimensional compositional simulator for steam injection processes". Ph. D Thesis, The Pennsylvania State University. (1990)

4. Jensen, T.B., "Steam flooding of fractured reservoirs: Experimental and numerical studies". Ph. D Thesis, University of Wyoming. (1991)
5. Mohamadi, M., Gong, X., and Wan, R.G., "Laboratory and Constitutive Modeling of Colorado Shale at High Pressure and Temperature". ARMA 13-651. 47th US Rock Mechanics/Geomechanics Symposium. San Francisco, CA, USA, June. (2013)
6. Rowe, P.W., "The stress-dilatancy relation for static equilibrium of an assembly of particles in contact". Proc. R. Soc. London. 269, pp. 500-527. (1962)
7. Shutler, N.D., "Numerical, Three-Phase Simulation of the Linear Steamflood Process". Society of Petroleum Engineers J., pp. 232-246. (1969)
8. Shutler, N.D., "Numerical Three-Phase Model for the Two-Dimensional Steamflood Process". Society of Petroleum Engineers J., pp. 365-376. (1970)
9. Wan, R.G., and Guo, P.J., "A Simple Constitutive Model for Granular Soils: Modified Stress-Dilatancy Approach". Computer and Geotechnics, Vol. 22, No. 2, pp. 109-133. (1998)
10. Wan, R.G., Pinheiro, M., and Guo, P.J., "Elastoplastic modelling of diffuse instability response of geomaterials". Int. J. Numer. Anal. Mech. Geomech, 35, pp. 140-160. (2011)
11. Wan, R.G., Pinheiro, M., Daouadji, A., Jrad, M., and Darve, F., "Diffuse instability with transition to localization in loose granular materials". Int. J. Numer. Anal. Mech. Geomech, Published on line, DOI: 10.1002/nag. 2085. (2012)